J Radioanal Nucl Chem (2011) 289:781–788
DOI 10.1007/s10967-011-1129-4

Sorption of uranium(VI) on Na-attapulgite as a function of contact time, solid content, pH, ionic strength, temperature and humic acid

**Wubiao Zhu · Zhengjie Liu · Lei Chen ·
Yunhui Dong**

Received: 19 April 2011 / Published online: 15 May 2011
© Akadémiai Kiadó, Budapest, Hungary 2011

Abstract Sorption of U(VI) from aqueous solution to Na-attapulgite was investigated at different experimental chemistry conditions by using batch technique. The attapulgite sample was characterized by FTIR and XRD. Sorption of U(VI) on attapulgite was strongly dependent on pH and ionic strength. The sorption of U(VI) on attapulgite increased quickly with rising pH at $pH < 6$, and decreased with increasing pH at $pH > 7$. The presence of humic acid (HA) enhanced the sorption of U(VI) on attapulgite obviously at low pH because of the strong complexation of surface adsorbed HA with U(VI) on attapulgite surface. Sorption of U(VI) on attapulgite was mainly dominated by ion exchange and/or outer-sphere surface complexation at low pH values, whereas the sorption was attributed to the inner-sphere surface complexation or precipitation at high pH values. The sorption increased with increasing temperature and the thermodynamic parameters calculated from the temperature dependent sorption isotherms suggested that the sorption of U(VI) on attapulgite was a spontaneous and endothermic process. The results indicate that attapulgite is a very suitable material for the preconcentration of U(VI) ions from large volumes of aqueous solutions.

Keywords Attapulgite · U(VI) · Sorption · pH · Ionic strength · Temperature

W. Zhu (✉)
Department of Industry Analysis, College of Zhongshan Polytechnic, Zhongshan 528404, Guangdong,
People's Republic of China
e-mail: zhuwb7812@163.com

Z. Liu · L. Chen · Y. Dong
School of Chemical Engineering, Shandong University of Technology, Zibo 255049, Shandong,
People's Republic of China

Introduction

The physicochemical behavior of long-lived lanthanides and actinides has aroused great interest in terms of the radioactive waste disposal [1–5]. To assess the actinides' behavior in the natural environment, the sorption, migration and diffusion of actinides in natural minerals and oxides are of paramount importance [6–8]. The fate of radionuclides in the environment is generally controlled by sorption reactions, complexation, and colloid formation with minerals [9–13]. Uranium is a very important element in the context of radioactive disposals because it is the major waste component, and together with its daughter products, can significantly contribute to the radiological impact. In the last decade, sorption of U(VI) on different minerals and oxides has been studied extensively [14–25]. The results indicated that sorption of U(VI) is strongly dependent on pH and ionic strength. The sorption increases from almost zero at low pH to the highest sorption at neutral pH, and then decreases again with pH increasing. However, the thermodynamic study of U(VI) on minerals and oxides is still not enough, which is crucial for the evaluation of the environmental behavior of U(VI) in the natural environment.

Uranium occurs naturally as U isotopes, ^{238}U (99.28%), ^{235}U (0.711%) and ^{234}U (0.006%), and they exist as hexavalent uranyl complex in the natural environment. The use of uranium at industrial and military sites has resulted in very high uranium contamination, and dangerous to human healthy and environmental protection because of its long half-life (such as $^{238}U\ t_{1/2} = 4.51 \times 10^9$ years). Attapulgite $[(Mg,Al)_4(Si)_8(O,OH,H_2O)_{26}\cdot nH_2O]$ is a hydrated magnesium aluminum silicate present in nature as fibrillar mineral [26–28]. The permanent negative surface charge enables it to adsorb heavy metal ions and radionuclides from aqueous solutions. In the last decade, attapulgite has been investigated as an adsorbent in the removal of organic contaminants, heavy metal ions and radionuclides from aqueous solutions by using batch and spectroscopy techniques [26–29]. Fan et al. [29] studied Eu(III) sorption on attapulgite by using EXAFS spectroscopy and found that the microstructure of Eu(III) adsorbed on attapulgite was affected by pH and humic acid (HA). Humic substances (HSs) are ubiquitous in soils, sediments, and natural waters. HSs are a complex mixture of organic compounds and may profoundly affect the physicochemical and biological behavior of radionuclides in the subsurface [30]. The influence of HSs on the sorption of radionuclides on minerals, nanomaterials and oxides has been studied intensively in the last decade [31–37]. The results indicated that the presence of HSs enhances the sorption of radionuclides at low pH and reduces the sorption at high pH values. The increase of sorption is explained by the sorption of HSs on the mineral surface followed by the interaction of the radionuclides with surface adsorbed HSs, whereas the reduction of sorption is explained by the formation of soluble radionuclide-HS complexes in aqueous solution which stabilize the radionuclides in solutions.

To our best knowledge, the sorption of U(VI) on attapulgite is still scarce, especially the effect of temperature on U(VI) sorption. In this work, the attapulgite was used as adsorbent to remove U(VI) ions from large volumes of aqueous solutions. The sorption of U(VI) on attapulgite was studied as a function of contact time, solid content, pH, ionic strength, HA and temperature by using batch technique. The sorption mechanism of U(VI) on attapulgite was discussed in detail.

Experimental

Chemicals

All chemicals used in the experiments were purchased in analytical purity and used without any purification. The attapulgite sample was derived from KaiXi Co. (Gansu, China). The sample was treated with 5% hydrochloric acid for 24 h, then was immersed into 20% NaCl solution for 60 h; and rinsed with distilled water until no Cl^- was detected with 0.01 M $AgNO_3$. Thus achieved attapulgite sample was dried at 105 °C for 2 h to eliminate the free adsorbed water, and was milled and passed through a 320-mesh screen. The N_2-BET surface area was 101 m^2/g.

U(VI) stock solution was prepared by dissolving uranyl nitrate hexahydrate ($UO_2(NO_3)_2 \cdot 6H_2O$) in Milli-Q water. The stock solution was kept at pH 3 and used in the following sorption experiments. Soil HA was extracted from the soil of Gansu province (China). The main elements are: C 60.44%, H 3.53%, N 4.22%, O 31.31% and S 0.50% [38, 39].

Sorption experiments

All the sorption experiments were carried out under ambient conditions. Stock suspensions of attapulgite and NaCl were contacted for 24 h to achieve the equilibrium of Na^+ with attapulgite, and then U(VI) stock solution was added in the polyethylene tubes to achieve the desired concentrations of different components. The pH values were adjusted by adding negligible volumes of 0.1 or 0.01 M HCl or NaOH. After the suspensions were shaken for 2 days, the solid phase was separated from the aqueous solution by centrifugation at 6,000 rpm for 30 min at controlled temperature same to that in sorption experiments. The concentration of U(VI) in the supernatant was analyzed by Arsenazo III spectrophotometric method at wavelength of 650 nm. All the experimental data were the average of duplicate determinations, and the average uncertainties were <5%.

XRD and FTIR analysis

The surface properties of attapulgite were characterized by Fourier Transform Infrared spectroscopy (FTIR) and X-ray diffraction (XRD). The FTIR spectrum was mounted on a BrukerEQUINOX55 spectrometer (Nexus) in KBr pellet at room temperature. The XRD pattern was obtained from a D/Max-rB equipped with a rotation anode using Cu K_α radiation ($\lambda = 0.15406$ nm). The XRD device was operated at 40 kV and 80 mA. The measurements were carried out in the range of $5° \leq 2\theta \leq 70°$.

Results and discussion

XRD and FTIR characterization

Figure 1 shows the XRD pattern of the attapulgite sample. The peak positions ($2\theta = 8.4°$, 19.7°, 25.4°, 27.5°, 34.6° and 42.6°) correspond to the crystal structure of attapulgite. The peak at $2\theta = 8.4°$ has the interplanar distance of $d = 1.064$ nm which is attributed to the basal plane of attapulgite structure [26, 27]. The intergrowth-minerals of montmorillonite and quartz are also found in the attapulgite sample, and are also marked in Fig. 1.

Figure 2 shows the FTIR spectrum of attapulgite sample. The peak at 3,620 cm^{-1} corresponds to the stretching vibration of Al–OH unite and the peak at 3550 cm^{-1} corresponds to Fe–OH unite. The broad band at 3,420 cm^{-1} is due to the H-OH vibration of the water molecules adsorbed on the solid surface. The peak at 1,650 cm^{-1} is attributed

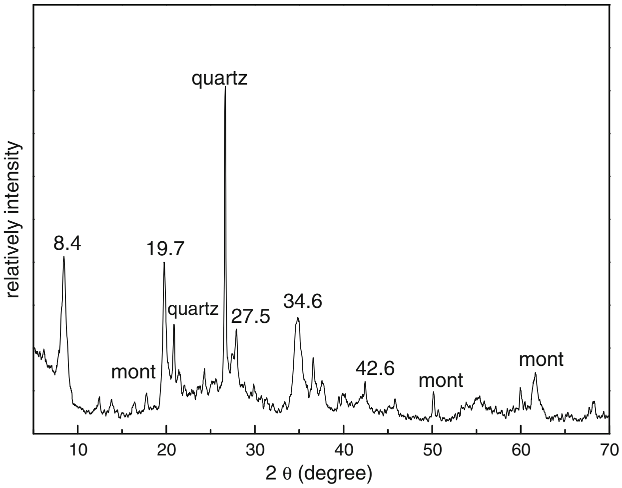

Fig. 1 XRD pattern of Na-attapulgite sample

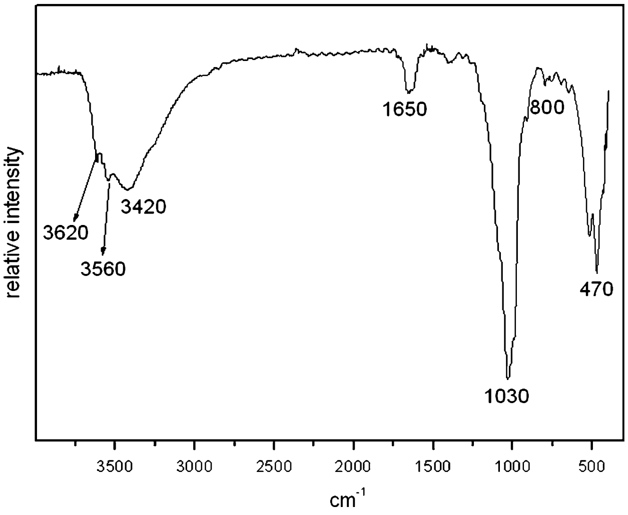

Fig. 2 FTIR spectrum of Na-attapulgite sample

to the bend vibration of zeolitic water. The peaks at 1,030 cm^{-1} and 470 cm^{-1} are attributed to Si–O–Si bonds. The peak at 800 cm^{-1} corresponds to the stretching vibration of Al–O–Si [40, 41].

Effect of contact time

Figure 3 shows the effect of contact time on U(VI) sorption to attapulgite. The sorption of U(VI) on attapulgite was quickly and a contact time of 5 h was enough to achieve sorption equilibrium. The sorption was initially fast in the first contact time, and then increased slowly in the following contact time. This two-step sorption process follows the general behavior of metal ion sorption at solid-water interfaces [42]. The interaction of U(VI) with surface sites of attapulgite is fast, and then the slow continued U(VI) sorption at attapulgite includes sorption of U(VI) ions onto sites that have relatively large activation energies, diffusion into the micropores of attapulgite, and a continuous growth of a surface precipitate [43, 44]. According to the above results, the shaking time was fixed to 24 h in the following experiments to assure the sorption equilibrium.

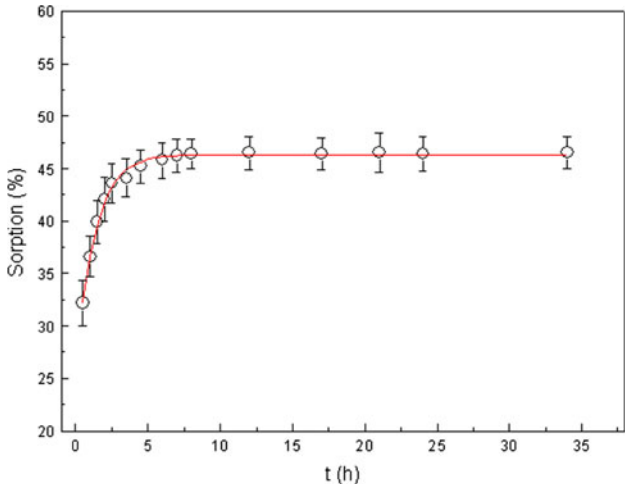

Fig. 3 Effect of contact time on the sorption of U(VI) to Na-attapulgite. $m/V = 1.0$ g/L, $I = 0.01$NaCl, pH = 4.4 ± 0.1, $T = 20 \pm 1$ °C, $C[\mathrm{U(VI)}]_{\mathrm{initial}} = 1.5 \times 10^{-6}$ mol/L

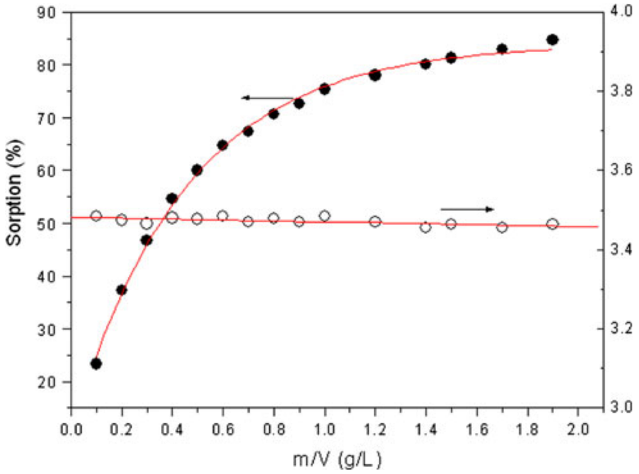

Fig. 4 Effect of solid content on the sorption of U(VI) to Na-attapulgite. $I = 0.01$NaCl, pH = 5.0 ± 0.1, $T = 20 \pm 1$ °C, $C[\mathrm{U(VI)}]_{\mathrm{initial}} = 1.5 \times 10^{-6}$ mol/L

Effect of solid content

The effect of solid content on U(VI) sorption to attapulgite is shown in Fig. 4. It can be seen that the removal percentage of U(VI) from aqueous solution to attapulgite increases with increasing solid content. This is to be expected because, for a fixed initial U(VI) concentration, increasing attapulgite content can provide more sorption sites and thereby increases the sorption of U(VI) on attapulgite. From Fig. 4, it is obvious that the distribution coefficient (K_d) decreases weakly with increasing solid contents. This may be attributed to the following factors: [1] A higher solid content effectively reduces the unsaturation of the sorption sites and accordingly, the number of such sites per unit mass comes down resulting in comparatively less sorption at higher solid amount; (2) At the low solid content, the U(VI) ions can easily access the sorption sites and thus results in the high K_d values; (3) Higher solid content creates particle aggregation, which can result in a decrease in the total surface area of solid and an increase in diffusion path length which leads to the decrease in sorption amount [45, 46]. The K_d values are quite in consistent with the physicochemical properties of K_d, i.e., K_d values are independent of solid contents at very low solid contents, and decrease with increasing solid content at high solid contents.

Effect of pH and ionic strength

Sorption of U(VI) on attapulgite in 0.001, 0.01 and 0.1 M NaCl solutions, respectively, in the pH range of 2–11 is shown in Fig. 5. It is clear that the sorption of U(VI) on attapulgite is strongly dependent on pH and ionic strength. Sorption of U(VI) increases quickly at pH 3–6, reaches the maximum sorption at pH 6–7, and then decreases with increasing pH at pH > 7. The pH dependent sorption of U(VI) on attapulgite suggests that the sorption is attributed to surface complexation. The strong pH dependent sorption of U(VI) can be interpreted from the species of U(VI) in solution. The hydrolysis constants of U(VI) are listed in Table 1 [47]. The relative species of U(VI) as a function of pH values are shown in Fig. 6. At pH < 4, UO_2^{2+} is the mainly species (>99%); at pH 5–6, the main species are UO_2^{2+}, $UO_2(OH)^+$, $UO_2(OH)_2^0$ and UO_2CO_3. At pH > 7, the prominent species are $UO_2(CO_3)_2^{2-}$ and UO_2CO_3. Wazne et al. [48] studied uranium(VI) sorption by iron oxyhydroxide, and found U(VI) presented mainly as $UO_2(OH)^+$, $(UO_2)_3(OH)_7^+$ and $(UO_2)_5(OH)_7^+$ at a neutral pH range in the absence of carbonate; however, the prominent species were uranyl carbonate at pH > 5 in the presence of carbonate.

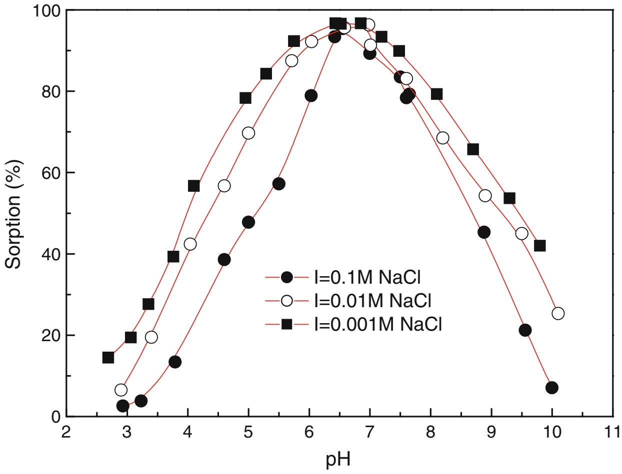

Fig. 5 Sorption of U(VI) on Na-attapulgite in different NaCl solutions as a function of pH values. $m/V = 1.0$ g/L, $T = 20 \pm 1$ °C, $C[U(VI)]_{initial} = 1.5 \times 10^{-6}$ mol/L

Table 1 Reaction and parameters used in the model calculations [47]

Species	Reaction	Log *K*
UO_2OH^+	$H_2O + UO_2^{2+} \leftrightarrow H^+ + UO_2OH^+$	−5.89
$UO_2(OH)_2^0$	$2H_2O + UO_2^{2+} \leftrightarrow 2H^+ + UO_2(OH)_2$ (aq)	−12.0
$UO_2(OH)_3^-$	$3H_2O + UO_2^{2+} \leftrightarrow 3H^+ + UO_2(OH)_3^-$	−20.0
$UO_2(OH)_4^{2-}$	$4H_2O + UO_2^{2+} \leftrightarrow 4H^+ + UO_2(OH)_4^{2-}$	−33.0
$UO_2(CO_3)^0$	$UO_2^{2+} + CO_3^{2-} \leftrightarrow UO_2CO_3$ (aq)	9.6
$UO_2(CO_3)_2^{2-}$	$UO_2^{2+} + 2CO_3^{2-} \leftrightarrow UO_2(CO_3)_2^{2-}$	16.9
$UO_2(CO_3)_3^{4-}$	$UO_2^{2+} + 3CO_3^{2-} \leftrightarrow UO_2(CO_3)_3^{4-}$	21.6
H_2CO_3	$2H^+ + CO_3^{2-} \leftrightarrow H_2CO_3$ (aq)	16.681
H_2O	$H_2O \leftrightarrow H^+ + OH^-$	13.8

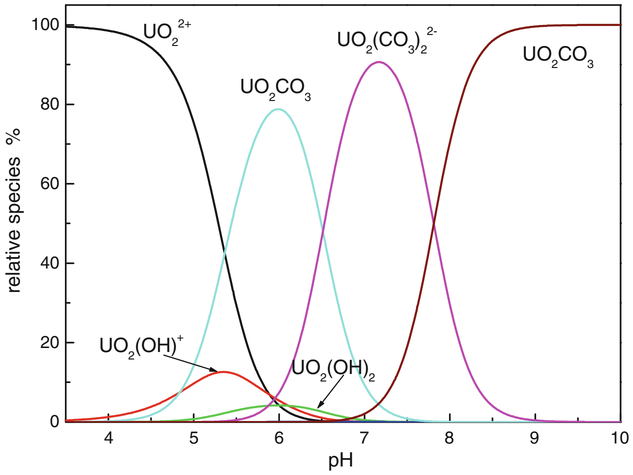

Fig. 6 The relative species of U(VI) as a function of pH in aqueous solutions in the presence of CO_2, $pCO_2 = 3.16 \times 10^{-4}$ atm

The decreasing of U(VI) sorption on attapulgite at pH > 7 may be explained in terms of zero point of charge (pH_{zpc}) of attapulgite and the species of U(VI). The surface charge of attapulgite is negative at pH > pH_{zpc}. The electrostatic repulsion between $UO_2(CO_3)_2^{2-}$ and negative surface of attapulgite becomes strong with increasing pH at pH > pH_{zpc}, and thereby reduces the sorption of U(VI) on attapulgite at high pH values. Similar results were also found in the sorption of U(VI) on phyllite [49].

From Fig. 5, one can see that the removal of U(VI) is the highest in 0.001 M NaCl solution, and lowest in 0.1 M NaCl solution. The ionic strength dependent sorption suggests that ion exchange contributes to the sorption of U(VI) from aqueous solution to attapulgite. This indicates that ion exchange also contributes U(VI) sorption on attapulgite. The sorption of U(VI) is mainly via ion exchange with hydrogen and sodium ions that saturate the exchange sites [27, 50, 51]. The exchange can be expressed by the following reactions:

(1) Exchange with hydronium ions:

$$\equiv \mathrm{SOH} + \mathrm{UO}_2^{2+} \rightarrow \equiv \mathrm{SOUO}_2^{2+} + \mathrm{H}^+ \quad (1)$$

$$2 \equiv \mathrm{SOH} + \mathrm{UO}_2^{2+} \rightarrow (\equiv \mathrm{SO})_2\mathrm{UO}_2^{2+} + 2\mathrm{H}^+ \quad (2)$$

$$\equiv \mathrm{SOH}_2^+ + \mathrm{UO}_2^{2+} \rightarrow \equiv \mathrm{SOHUO}_2^{2+} + \mathrm{H}^+ \quad (3)$$

$$2 \equiv \mathrm{SOH}_2^+ + \mathrm{UO}_2^{2+} \rightarrow (\equiv \mathrm{SOH})_2\mathrm{UO}_2^{2+} + 2\mathrm{H}^+ \quad (4)$$

(2) Exchange with Na^+ ions:

$$\equiv \mathrm{SONa} + \mathrm{UO}_2^{2+} \rightarrow \equiv \mathrm{SO} = \mathrm{UO}_2^{2+} + \mathrm{Na}^+ \quad (5)$$

(3) The hydrolysis of U(VI) in solution

$$\mathrm{UO}_2^{2+} + n\mathrm{H}_2\mathrm{O} \Leftrightarrow [\mathrm{UO}_2(\mathrm{H}_2\mathrm{O})_{n-m}]^{2-m} + m\mathrm{H}^+ \quad (6)$$

Being $n > m$, and exchange with hydrolyzed species:

$$\begin{aligned} &\equiv \mathrm{SOH} + \mathrm{UO}_2(\mathrm{OH})_m(\mathrm{H}_2\mathrm{O})_{n-m}^{2-m} \rightarrow \\ &\quad \equiv \mathrm{SOUO}_2(\mathrm{OH})_m^{1-m} + \mathrm{H}^+ + (n-m)\mathrm{H}_2\mathrm{O} \quad (7) \end{aligned}$$

The strong pH and ionic strength dependent sorption of U(VI) on attapulgite suggests that the sorption is dominated by surface complexation and ion exchange [52–54]. Generally, the strong pH dependent and ionic strength independent sorption is dominated by inner-sphere surface complexation, whereas the strong ionic strength dependent and pH independent sorption is dominated by outer-sphere surface complexation and ion exchange. Herein, the sorption of U(VI) on attapulgite is complicated.

Effect of HA

Figure 7 shows the sorption of U(VI) on attapulgite as a function of pH in the presence and absence of HA. At pH < 6, the presence of HA enhances the sorption of U(VI) on HA-attapulgite drastically. HA has a macromolecular structure, only a small fraction of the "sorbed" carboxylic and phenolic groups of HA directly interact with attapulgite surface sites and the remained "sorbed" groups are free to interact with metal ions [55]. The complexation of HA and U(VI) is stronger than that of U(VI) with functional groups on attapulgite surface. At low pH values, the HA molecules are adsorbed on attapulgite, and the surface adsorbed HA forms strong complexes with U(VI) on attapulgite surfaces and thereby enhances the sorption of U(VI) on HA-attapulgite hybrids. Compared to the sorption of U(VI) on attapulgite in the absence of HA, the sorption decreased slightly with increasing pH values at pH > 7. This is also attributed to the surface adsorbed HA on attapulgite, which forms strong complexes on attapulgite surfaces.

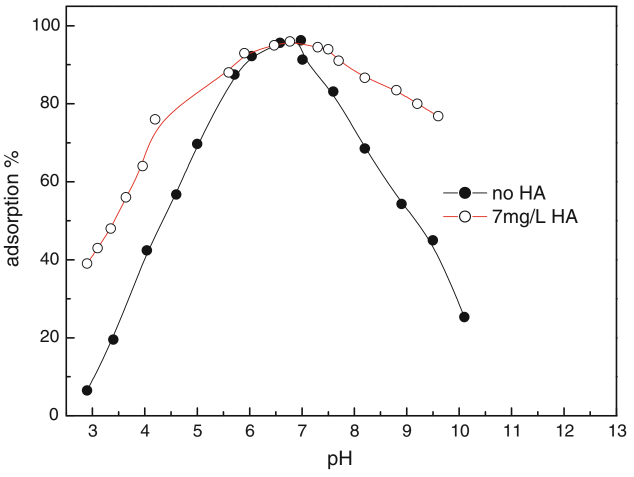

Fig. 7 Sorption of U(VI) on attapulgite as a function of pH values in the presence and absence of HA. $m/V = 1.0$ g/L, $I = 0.01$ NaCl, $T = 20 \pm 1$ °C, $C[\mathrm{U(VI)}]_{\mathrm{initial}} = 1.5 \times 10^{-6}$ mol/L

Sorption isotherms and thermodynamic parameters

The temperature is a very important parameter in the study of radionuclide sorption. Effect of temperature on sorption of U(VI) to attapulgite is shown in Fig. 8. One can see that the sorption isotherm is the highest at $T = 333.15$ K and is the lowest at $T = 293.15$ K, suggesting that the sorption of U(VI) on attapulgite increases with rise in temperature. The results indicate that high temperature is advantageous for U(VI) sorption on attapulgite. The sorption isotherms are simulated by Langmuir and Freundlich isotherm models and the results are shown in Fig. 8b, c.

The Langmuir model assumes that sorption occurs in a monolayer with all sorption sites identical and energetically equivalent. Its linear form can be described as [56]:

$$\frac{C_e}{C_s} = \frac{1}{bC_{s\max}} + \frac{C_e}{C_{s\max}} \quad (8)$$

where C_e is the equilibrium concentration of U(VI) remained in solution ($\mathrm{mol \cdot L^{-1}}$); C_s is the amount of U(VI) adsorbed on attapulgite after sorption equilibrium ($\mathrm{mol\ g^{-1}}$); $C_{s\ \max}$ is the maximum sorption capacity at complete monolayer coverage ($\mathrm{mol\ g^{-1}}$), and b ($\mathrm{L\ mol^{-1}}$) is a constant that relates to the heat of sorption.

The Freundlich model is an exponential equation with the assumption that the sorption occurs on the heterogeneous sorbent surface. The equation is represented as [56]:

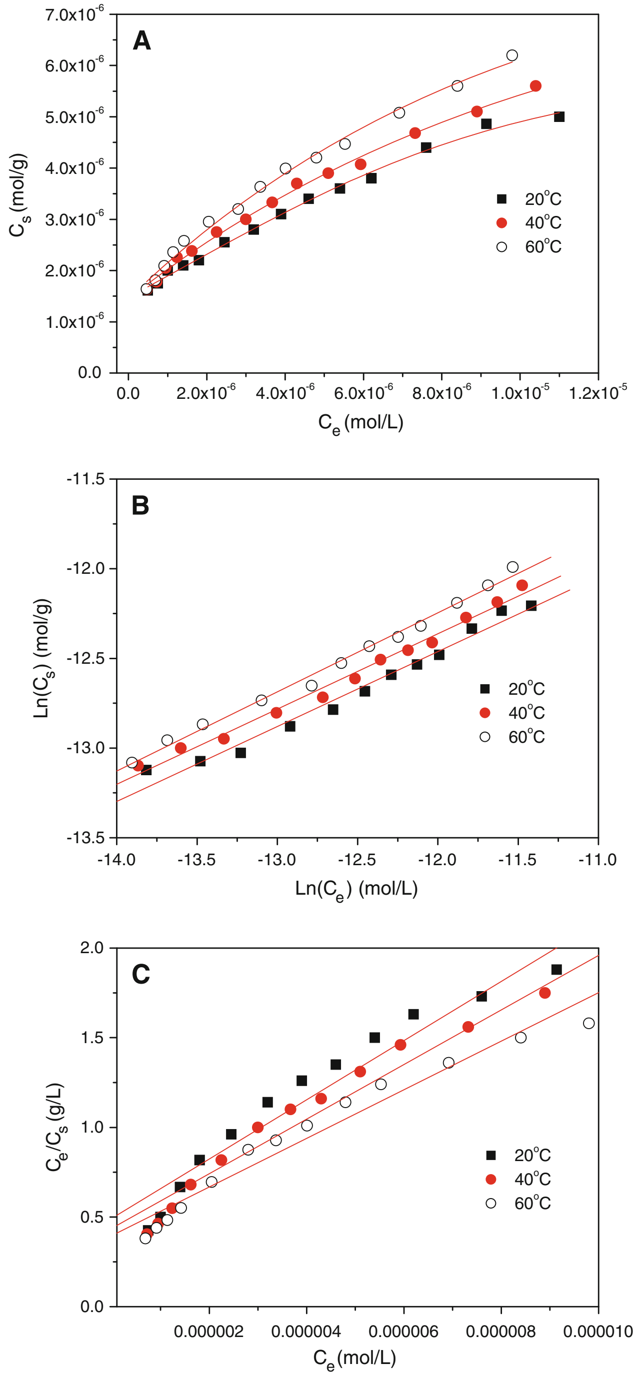

Fig. 8 Sorption isotherms of U(VI) on attapulgite at different temperatures. $m/V = 1.0$ g/L, pH $= 4.4 \pm 0.1$, $I = 0.01$NaClO$_4$. **a** Sorption isotherms; **b** Freundlich model simulation; **c** Langmuir model simulation

$$\ln C_s = \ln k_F + n \ln C_e \tag{9}$$

where k_F (mol^{1-n} L^n g^{-1}) represents the sorption capacity when metal ion equilibrium concentration equals to 1, and n represents the degree of sorption dependent with equilibrium concentration.

Table 2 The parameters for the Langmuir and Freundlich isotherm models of U(VI) sorption on attapulgite at different temperatures

Correlation parameters	$T = 293.15$ K	$T = 313.15$ K	$T = 333.15$ K
Langmuir			
$C_{s\ max}$ (mol g^{-1})	6.06×10^{-5}	6.57×10^{-5}	7.38×10^{-5}
b (L mol^{-1})	3.34×10^{5}	3.48×10^{5}	3.42×10^{5}
R^2	0.97	0.98	0.98
Freundlich			
k_F (mol^{1-n} L^n g^{-1})	6.65×10^{-4}	7.51×10^{-4}	1.08×10^{-3}
n	0.418	0.420	0.441
R^2	0.99	0.99	0.99

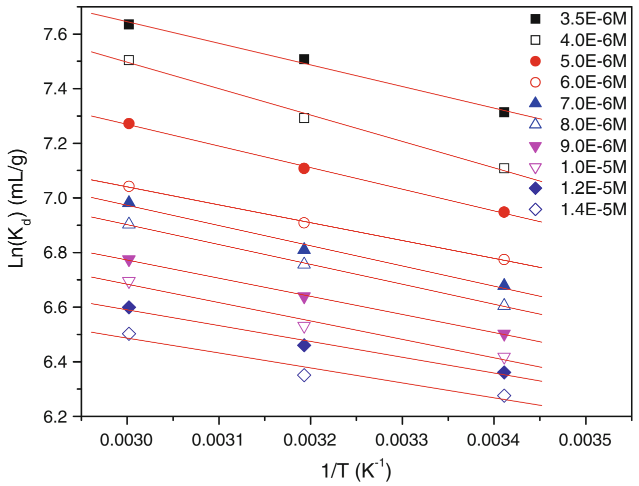

Fig. 9 Linear plots of LnK_d versus C_e at different temperatures and different initial U(VI) concentrations. $m/V = 1.0$ g/L, initial pH $= 4.4 \pm 0.1$, $I = 0.01$ M NaCl

The relative values calculated from the two models are listed in Table 2. As can be seen from Fig. 8b, c, the Freundlich model simulates the experimental data better than the Langmuir model, which is also supported by the good correlation coefficients in Table 2. The values of $C_{s\ max}$ obtained from the Langmuir model are the highest at $T = 333.13$ K and the lowest at $T = 293.13$ K, which indicates that the sorption process is enhanced with increasing temperature. The value of n calculated from the Freundlich model is from unity, indicating that a nonlinear sorption of U(VI) takes place on attapulgite surfaces.

The distribution coefficients as a function of temperature at different initial concentrations at $T = 293.15$, 313.15 and 333.15 K are shown in Fig. 9. The thermodynamic parameters of ΔH^0, ΔS^0 and ΔG^0 of U(VI) sorption on attapulgite can be calculated from the temperature dependent sorption isotherms. The values of standard enthalpy change (ΔH^0) and standard entropy change (ΔS^0) can be

Table 3 Thermodynamic parameters of U(VI) sorption on attapulgite

C_0 (mol L^{-1})	ΔH^0 (kJ mol^{-1})	ΔS^0 (J mol^{-1} K^{-1})	ΔG^0 (kJ mol^{-1})		
			293.15 K	313.15 K	333.15 K
3.5×10^{-6}	6.56	83.2	−17.84	−19.50	−21.16
4.0×10^{-6}	8.04	86.5	−17.31	−19.04	−20.76
5.0×10^{-6}	6.57	80.1	−16.92	−18.53	−20.13
6.0×10^{-6}	5.44	74.8	−16.50	−17.99	−19.49
7.0×10^{-6}	6.15	76.4	−16.24	−17.77	−19.3
8.0×10^{-6}	6.04	75.5	−16.08	−17.59	−19.1
9.0×10^{-6}	5.52	72.8	−15.83	−17.29	−18.74
1.0×10^{-5}	5.60	72.3	−15.61	−17.05	−18.50
1.2×10^{-5}	4.80	69.3	−15.50	−16.88	−18.26
1.4×10^{-5}	4.55	67.6	−15.27	−16.62	−17.97

calculated from the slope and y-intercept of the plot of $\ln K_d$ vs. $1/T$ (Fig. 9) using the following equations [57, 58]:

$$K_d = \frac{C_0 - C_e}{C_e} \times \frac{V}{m} \quad (10)$$

$$\ln K_d = \frac{\Delta S^0}{R} - \frac{\Delta H^0}{RT} \quad (11)$$

Gibbs free energy changes (ΔG^0) of specific adsorption are calculated from:

$$\Delta G^0 = \Delta H^0 - T\Delta S^0 \quad (12)$$

Relevant parameters calculated from Eqs. 11 and 12 are given in Table 3. The values of thermodynamic parameters provide an insight into the mechanism concerning the interaction of U(VI) on attapulgite. The values of ΔH^0 are positive, suggesting that the sorption process is endothermic. One possible interpretation of the endothermic process is that U(VI) ions are well solvated in water [57]. In order for U(VI) ions to adsorb on attapulgite surface, they are denuded of their hydration sheath to some extent, and this dehydration process needs energy. It is assumed that this energy of dehydration exceed the exothermicity of U(VI) ions attaching to attapulgite surface. The removal of water molecules from U(VI) ions is essentially an endothermic process, and the endothermicity of the desolvation process exceed the enthalpy of sorption to a considerable extent [59, 60]. The values of Gibbs free energy change (ΔG^0) are negative as expected for a spontaneous process. The decrease of ΔG^0 with rise of temperature indicates more efficient sorption at higher temperature. The U(VI) ions are readily desolvated at higher temperature, and thereby their sorption to attapulgite becomes more favorable. The positive values of entropy change (ΔS^0) reflect the affinity of attapulgite toward U(VI) ions in aqueous solutions and might suggest some structure changes.

Conclusion

In the light of the results of this work, the following conclusions can be drawn:

(I) Sorption of U(VI) on attapulgite is strongly dependent on pH and ionic strength. The sorption of U(VI) increases with increasing pH at $pH < 6$, and decreases with increasing pH at $pH > 7$. The sorption of U(VI) on attapulgite is attributed to outer-sphere surface complexation and/or ion exchange at low pH, and dominated by inner-sphere surface complexation or surface precipitates at high pH values.

(II) The presence of HA significantly enhances U(VI) sorption on HA-attapulgite hybrids. The surface adsorbed HA can form strong surface complexes with U(VI) on attapulgite surfaces.

(III) The sorption isotherm of U(VI) on attapulgite is well fitted by Freundlich isotherm model.

(IV) The attapulgite is a suitable material for the preconcentration and solidification of U(VI) ions from large volumes of aqueous solutions in radioactive waste management.

References

1. Tan XL, Fan QH, Wang XK, Grambow B (2009) Environ Sci Technol 43:3115
2. Chen CL, Wang XK, Nagatsu M (2009) Environ Sci Technol 43:2362
3. Shao DD, Xu D, Wang SW, Fan QH, Wu WS, Dong YH, Wang XK (2009) Sci China B 52:362
4. Tan XL, Wang XK, Geckeis H, Rabung Th (2008) Environ Sci Technol 42:6532
5. Tan XL, Fang M, Wang XK (2010) Molecules 15:8431
6. Chen CL, Wang XK (2007) Appl Geochem 22:436
7. Singh A, Ulrich KU, Giammar DE (2010) Geochim Cosmochim Acta 74:6324

8. Tan X, Chen C, Yu S, Wang X (2008) Appl Geochem 23:2767
9. Sheng GD, Hu J, Wang XK (2008) Appl Radiat Isot 66:1313
10. Tan XL, Hu J, Zhou X, Yu SM, Wang XK (2008) Radiochim Acta 96:487
11. Shao DD, Fan QH, Li JX, Niu ZW, Wu WS, Chen YX, Wang XK (2009) Microporous Mesoporous Mater 123:1
12. Chen CL, Hu J, Xu D, Tan XL, Meng YD, Wang XK (2008) J Colloid Interface Sci 323:33
13. Stewart BD, Mayes MA, Fendorf S (2010) Environ Sci Technol 44:928
14. Schlegel ML, Descostes M (2009) Environ Sci Technol 43:8593
15. Wieland E, Mace N, Dahn R, Kunz D, Tits J (2010) J Radioanal Nucl Chem 286:793
16. Kim JH, Lee HI, Yeon JW, Jung Y, Kim JM (2010) J Radioanal Nucl Chem 286:129
17. Das D, Sureshkumar MK, Koley S, Mithal N, Pillai CGS (2010) J Radioanal Nucl Chem 285:447
18. Ayata S, Aydinci S, Merdivan M, Binzet G, Kulcu N (2010) J Radioanal Nucl Chem 285:525
19. Gao L, Yang ZQ, Shi KL, Wang XF, Guo ZJ, Wu WS (2010) J Radioanal Nucl Chem 284:519
20. Shao DD, Jiang ZQ, Wang XK, Li JX, Meng YD (2009) J Phys Chem B 113:860
21. Shao DD, Hu J, Wang XK (2010) Plasma Process Polym 7:977
22. Yusan S, Aslani MAA, Turkozu DA, Aycan HA, Aytas S, Akyil S (2010) J Radioanal Nucl Chem 283:231
23. Ren XM, Wang SW, Yang ST, Li JX (2010) J Radioanal Nucl Chem 283:253
24. Zhang HX, Tang Q, Tao ZY (2009) J Radioanal Nucl Chem 279:855
25. Humelnicu D, Drochioiu G, Sturza MI, Cecal A, Popa K (2006) J Radioanal Nucl Chem 270:637
26. Fan QH, Shao DD, Hu J, Wu WS, Wang XK (2008) Surf Sci 602:778
27. Fan QH, Shao DD, Wu WS, Wang XK (2009) Chem Eng J 150:188
28. Giustetto R, Xamena FXL, Ricchiardi G, Bordiga S, Damin A, Gobetto R, Chierotti MR (2005) J Phys Chem B 109:19360
29. Fan QH, Tan XL, Li JX, Wang XK, Wu WS, Montavon G (2009) Environ Sci Technol 43:5776
30. Montavon G, Markai S, Andres Y, Grambow B (2002) Environ Sci Technol 36:3303
31. Tan XL, Fang M, Chen CL, Yu SM, Wang XK (2008) Carbon 46:1741
32. Tan XL, Fang M, Wang XK (2008) J Nanosci Nanotechnol 8:5624
33. Sheng GD, Li JX, Shao DD, Hu J, Chen CL, Chen YX, Wang XK (2010) J Hazard Mater 178:333
34. Li JX, Chen SY, Sheng GD, Hu J, Tan XL, Wang XK (2011) Chem Eng J 166:551
35. Hu J, Xu D, Chen L, Wang XK (2009) J Radioanal Nucl Chem 279:701
36. Xu D, Tan XL, Chen CL, Wang XK (2008) J Hazard Mater 154:407
37. Hu J, Chen CL, Zhu XX, Wang XK (2009) J Hazard Mater 162:1542
38. Tan XL, Fang M, Li JX, Lu Y, Wang XK (2009) J Hazard Mater 168:458
39. Hu J, Xie Z, He B, Sheng GD, Chen CL, Li JX, Chen YX, Wang XK (2010) Sci China B 53:1420
40. Yang ST, Li JX, Lu Y, Chen YX, Wang XK (2009) Appl Radiat Isot 67:1600
41. Zhao GX, Zhang HX, Fan QH, Ren XM, Li JX, Chen YX, Wang XK (2010) J Hazard Mater 173:661
42. Lee S, Anderson PR, Bunker GB, Karanfil C (2004) Environ Sci Technol 38:5426
43. Strathmann TJ, Myneni SB (2005) Environ Sci Technol 39:4027
44. Sheng GD, Hu J, Jin H, Yang ST, Ren XM, Li JX, Chen YX, Wang XK (2010) Radiochim Acta 98:291
45. Yang X, Yang SB, Yang ST, Hu J, Tan XL, Wang XK (2011) Chem Eng J 168:86
46. Hu BW, Cheng W, Zhang H, Sheng GD (2010) J Radioanal Nucl Chem 285:389
47. Niu ZW, Fan QH, Wang WH, Xu JZ, Chen L, Wu WS (2009) Appl Radiat Isot 67:1582
48. Wazne M, Korfiatis G, Meng X (2003) Environ Sci Technol 37:3619
49. Arnold T, Zorn T, Zänker H, Bernhard G, Nitsche H (2001) J Contam Hydrol 47:219
50. Hu J, Shao DD, Chen CL, Sheng GD, Li JX, Wang XK, Nagatsu M (2010) J Phys Chem B 114:6779
51. Chen CL, Hu J, Shao DD, Li JX, Wang XK (2009) J Hazard Mater 164:923
52. Lu SS, Guo ZQ, Zhang CC, Zhang SW (2011) J Radioanal Nucl Chem 287:621
53. Zuo LM, Yu SM, Zhou H, Tian X, Jiang J (2011) J Radioanal Nucl Chem 288:379
54. Zhang SW, Guo ZQ, Xu JZ, Niu HH, Chen ZS, Xu JZ (2011) J Radioanal Nucl Chem 288:121
55. Chen CL, Wang XK, Jiang H, Hu WP (2007) Colloid Surf A 302:121
56. Sheng GD, Shao DD, Fan QH, Xu D, Chen YX, Wang XK (2009) Radiochim Acta 97:621
57. Sheng GD, Wang SW, Hu J, Lu Y, Li JX, Dong YH, Wang XK (2009) Colloid Surface A 339:159
58. Xu D, Zhou X, Wang X (2008) Appl Clay Sci 39:133
59. Zuo LM, Yu SM, Zhou H, Jiang J, Tian X (2011) J Radioanal Nucl Chem 288:579
60. Chen CL, Wang XK (2006) Ind Eng Chem Res 45:9144